I&EC research
Industrial & Engineering Chemistry Research
pubs.acs.org/IECR
Article

Glucosamine for CO_2 Capture: Absorption Kinetics, Promoted Absorption Rate, and Comparison with Other Amino Sugars

Urvashi K. Sarode, Prakash D. Vaidya,* and Eugeny Y. Kenig

Cite This: *Ind. Eng. Chem. Res.* 2023, 62, 1492−1498
Read Online
ACCESS | Metrics & More | Article Recommendations | Supporting Information

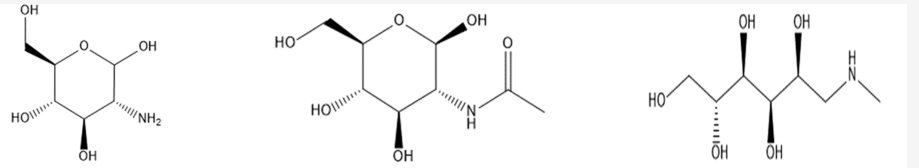

ABSTRACT: Amino sugars—sugars wherein the amine group substitutes the hydroxyl group—are renewable and ecofriendly CO_2 separation solvents. In this work, the kinetics of CO_2 absorption in the amino sugar glucosamine (GA) was studied. Absorption rates in aqueous GA solutions (0.1−1 M) were measured in a stirred cell reactor in the 303−313 K range. At T = 308 K, the value of the reaction rate constant for GA (0.1 M) was 27 M^{-1} s^{-1}. The two-step zwitterion mechanism was employed for describing the reaction pathway. Some useful characteristics of GA solutions, such as density and viscosity, were measured. Using the modified Stokes law and the N_2O analogy method, the diffusivity and solubility of CO_2 in solutions were determined. The liquid-side mass-transfer coefficient was found to be 0.005 cm/s at 308 K. Three amine promoters were chosen to improve the reactivity of GA, viz., monoethanolamine (MEA), 2-amino-2-methyl-1-propanol (AMP), and piperazine (PZ). Mixtures of GA/PZ (2.5/0.5 M) were the most reactive. The reactivity of two further amino sugars, *N*-acetyl-D-glucosamine (NAG) and *N*-methyl-D-glucamine (NMG), was also studied, and a comparison with GA was provided. NMG was the most reactive with CO_2, whereas GA was the least reactive. This work will draw attention to this new category of CO_2-capturing solvents.

1. INTRODUCTION

Absorbents derived from natural sources are promising for CO_2 capture because they are renewable and ecofriendly. Amino sugars, which occur widely in nature, represent a candidate class of benign CO_2 separation solvents. Glucosamine (GA), *N*-acetyl-D-glucosamine (NAG), and *N*-methyl-D-glucamine (NMG) are examples of this category of reagents (see Figure 1). GA ($C_6H_{13}NO_5$) is a hexosamine made from glucose and is found in chitin, chitosan, and polysaccharides. An amino group substitutes the hydroxyl group in this weakly basic sugar, thereby suggesting the possibility to react with absorbed CO_2 in the liquid phase.

Navaza's research group put forth the idea of using GA as a CO_2-capturing solvent due to its nontoxicity and ease of biodegradation.[1−4] For example, Gomez-Diaz et al.[1] investigated the gas−liquid mass-transfer process for the CO_2−glucose and CO_2−GA systems in aqueous solutions using a cylindrical bubble column. They established the dependence of mass-transfer coefficient on the composition of the liquid phase. In another work,[2] they found that the CO_2−GA reaction in aqueous solutions was moderately fast. Besides, they reported that the gas−liquid interfacial area increased with the rising CO_2 gas flow rate, whereas the mass-transfer coefficient reduced with the rising free GA concentration in the liquid phase. Gomez-Diaz and Navaza[3] studied chemical reaction kinetics in a stirred reactor with a flat gas−liquid interface and established first-order kinetics for CO_2 and GA.

It was found that the activation energy (47 kJ mol^{-1}) was close to the activation energy (E_{act}) values for the reactions of CO_2 with amines such as MEA (monoethanolamine). A certain steric hindrance for the CO_2−GA reaction was suggested. Finally, Garcia-Abuin et al.[4] performed ^{13}C NMR studies and found that bicarbonate ions were produced during the reactive absorption of CO_2 in aqueous GA solutions. The CO_2−amino sugar reaction stoichiometry was 1:1, thereby suggesting that these sugars were loading CO_2. However, GA degraded fast at high temperatures, and thus milder methods were necessary for regenerating amino sugars.

Both GA and NAG react moderately fast with CO_2. There are few works that report the values of their second-order rate constant (k_2) and E_{act} in diluted solutions. For instance, $k_{2,GA}$ equals 10 M^{-1} s^{-1} at T = 298 K in the 50−400 mM range of GA

Received: July 31, 2022
Revised: December 9, 2022
Accepted: December 30, 2022
Published: January 17, 2023

https://doi.org/10.1021/acs.iecr.2c02745
Ind. Eng. Chem. Res. 2023, 62, 1492−1498

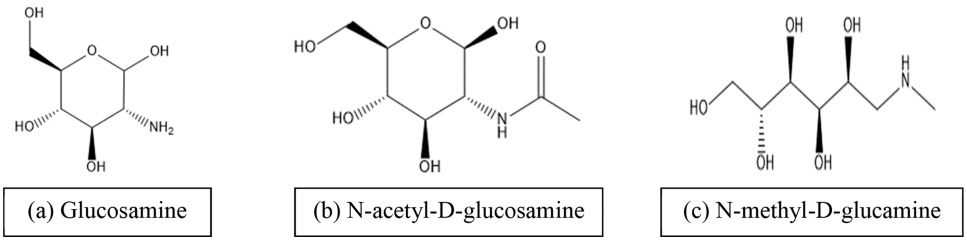

Figure 1. Molecular structure of glucosamine, *N*-acetyl-D-glucosamine and *N*-methyl-D-glucamine.

concentrations, according to Gomez-Diaz and Navaza,[3] and E_{act} equals 47 kJ mol^{-1}. In our recent work with weak NAG solutions (20−100 mM),[5] it was shown that the value for $k_{2,NAG}$ was higher (125 M^{-1} s^{-1} at T = 308 K), whereas E_{act} was lower (42 kJ mol^{-1}). Clearly, amino sugars were less reactive than other traditional solvents. It appeared helpful to add rate activators such as MEA, AMP (2-amino-2-methyl-1-propanol), and PZ (or piperazine) to NAG.[5]

It is interesting to augment the scarcely available data on the performance of amino sugars, especially at higher molarity and temperature; this was done in our work. First, chemical kinetics of GA (0.1−1 M) was studied in a stirred cell in the 303−313 K range. In future, the measured kinetics data may be used to develop a comprehensive numerical kinetic model. For instance, Liu et al.[6] developed a reaction kinetic model of CO_2 absorption into a new tertiary amine 1DMA2P (1-dimethylamino-2-propanol) using a FEM-based COMSOL software. Next, performance of concentrated GA/promoter mixtures (2.5/0.5 M) was investigated while MEA, AMP, and PZ were used as promoters. Furthermore, the reactivity of GA was compared with that of NAG (studied earlier[5]) and a third amino sugar compound NMG. NMG ($C_7H_{17}NO_5$), also known as meglumine, is a glucose-derived hexosamine and a secondary amine. The hydroxyl group at the first position in NMG is replaced with the nitrogen of a methylamino group (see Figure 1). NMG is a crystalline base, used together with iodinated organic compounds as the contrast medium. It is also applied in the pharmaceutical industry. The absorption of CO_2 into aqueous NMG is hitherto not reported in the literature. Surely, this work will accentuate the useful properties of this category of hexosamines. Especially, the outcomes will be helpful for a detailed analysis of the application of new CO_2-capturing solvents using commercial process software. In this regard, we can mention, for example, a rigorous simulation of absorption in potassium taurate performed by Moioli et al.[7] using ASPEN Plus. In another work, Moioli and Pellegrini[8] applied such simulations to analyze the solvent storage mode for the flexible operation of the CO_2 removal section in a natural gas-combined cycle power plant.

Besides, we provided new data on the physical properties of glucosamine and determined the mass-transfer coefficient in a stirred cell reactor. Today, artificial neural network (ANN) models can describe the physical properties of CO_2-capturing solvents. Thus, Liu et al.[9] developed such models to describe the experimental results of the physical properties of 1DMA2P. In another work, Quan et al.[10] developed generic AI models for predicting the mass-transfer coefficient in an amine-based CO_2 absorber. The present work will be useful for such forthcoming investigations on amino sugars.

2. THEORY

2.1. Reaction Pathway. The pathway for the CO_2 reactions with GA, NAG, and NMG is briefly summarized in this section. Unlike GA that comprises a primary amino group, both NAG and NMG are secondary amines. Amino sugars (or AsH) form unstable carbamates as per the zwitterion mechanism:[11−13]

$$CO_2 + AsH \overset{k_2,k_{-1}}{\longleftrightarrow} AsH^+COO^- \quad (1)$$

$$AsH^+COO^- + B \overset{\hat{k}_B}{\rightarrow} AsCOO^- + BH^+ \quad (2)$$

The base B in eq 2 can be AsH, H_2O, and OH^-. For the case when B is the amino sugar, the overall reaction for carbamate formation is represented by

$$CO_2 + 2AsH \leftrightarrow AsCOO^- + AsH_2^+ \quad (3)$$

Unstable carbamates, such as those formed by GA, NAG, and NMG, are fast hydrolyzed, and bicarbonate is formed as follows:

$$AsCOO^- + H_2O \leftrightarrow AsH + HCO_3^- \quad (4)$$

AsH forms bicarbonate instead of carbamate, according to Garcia-Abuin et al.:[4]

$$CO_2 + AsH + H_2O \leftrightarrow AsH_2^+ + HCO_3^- \quad (5)$$

As CO_2 reactions with H_2O and OH^- do not contribute to the overall rate,[3] R_{CO_2} is given by:

$$R_{CO_2} = \frac{k_2(CO_2)(AsH)}{1 + \frac{k_{-1}}{\hat{k}_B(B)}} = \frac{k_2(CO_2)(AsH)}{1 + \frac{k_{-1}}{\hat{k}_{AsH}(AsH) + \hat{k}_{H_2O}(H_2O) + \hat{k}_{OH^-}(OH^-)}} \quad (6)$$

The term $\hat{k}_B(B)$ in eq 6 represents the contribution of base B in zwitterion deprotonation.

2.2. Reaction Kinetics. In the bulk liquid, CO_2 concentrations were very low and hence could be neglected. Doraiswamy and Sharma[14] showed that the rate for the fast reaction regime is given by eq 7:

$$R_{CO_2} = k_L(CO_2)E \quad (7)$$

Here, (CO_2) is the saturation concentration of CO_2, and $k_L(CO_2)$ is the absorption rate for the diffusion controlled regime. The value of the enhancement factor (E) due to the reaction is given by the Hatta number:

$$Ha = \frac{\sqrt{\frac{2}{(m+1)}D_{CO_2}k_{m,n}(CO_2)^{m-1}(AsH)^n}}{k_L} \quad (8)$$

The kinetic parameters in eq 8 are the rate constant ($k_{m,n}$) and the reaction orders (m and n for CO_2 and AsH). To conform to

https://doi.org/10.1021/acs.iecr.2c02745
Ind. Eng. Chem. Res. 2023, 62, 1492−1498

Table 1. Physicochemical Properties of Aqueous GA Solutions

temperature (K)	concentration (M)	ρ (kg/m^3)	μ (mPa s)	$D_{CO_2} \times 10^9$ (m^2/s)	$H_{CO_2} \times 10^4$ (kmol/m^3 kPa)
303	0.5	1049	0.683	2.54	1.93
308	0.1	1006.3	0.604	2.79	1.96
308	0.3	1025	0.636	2.68	1.91
308	0.5	1046.4	0.667	2.58	1.88
308	1	1093.6	0.785	2.26	1.84
313	0.5	1044	0.654	2.79	1.79

the fast regime, the condition to be satisfied is $10 < \mathrm{Ha} \ll (E_i - 1)$. Here, E_i is the instantaneous enhancement factor, whose value as per the film theory is:

$$E_i = 1 + \left[\frac{(\mathrm{AsH})}{z(\mathrm{CO_2})}\frac{D_{\mathrm{AsH}}}{D_{\mathrm{CO_2}}}\right] \quad (9)$$

D_{AsH} denotes the diffusivity of AsH in liquid, whereas z denotes the stoichiometric reaction coefficient. It follows from eqs 7 and 8 that the reaction rate is given by:

$$R_{\mathrm{CO_2}} = \sqrt{\frac{2}{m+1} D_{\mathrm{CO_2}} k_{m,n} (\mathrm{CO_2})^{m+1} (\mathrm{AsH})^n} \quad (10)$$

It is known from Henry's law that $(\mathrm{CO_2}) = P_{\mathrm{CO_2}} H_{\mathrm{CO_2}}$. As $m = 1$, eq 10 is rewritten as:

$$R_{\mathrm{CO_2}} = P_{\mathrm{CO_2}} H_{\mathrm{CO_2}} \sqrt{D_{\mathrm{CO_2}} k_{1,n} (\mathrm{AsH})^n} \quad (11)$$

Upon rearranging and taking logarithm on both sides, we get:

$$\log\left\{\frac{R_{\mathrm{CO_2}}}{P_{\mathrm{CO_2}} H_{\mathrm{CO_2}} \sqrt{D_{\mathrm{CO_2}}}}\right\} = \left\{\frac{1}{2}\log(k_{1,n})\right\} + \left\{\frac{n}{2}\log(\mathrm{AsH})\right\} \quad (12)$$

If the variation in $R_{\mathrm{CO_2}}$ versus (AsH) is studied, a plot of $\log\left\{\frac{R_{\mathrm{CO_2}}}{P_{\mathrm{CO_2}} H_{\mathrm{CO_2}} \sqrt{D_{\mathrm{CO_2}}}}\right\}$ vs log(AsH) can provide the values of $k_{1,n}$ and n. For the first-order kinetics of AsH (i.e., $n = 1$), eq 11 further simplifies to

$$R_{\mathrm{CO_2}} = P_{\mathrm{CO_2}} H_{\mathrm{CO_2}} \sqrt{D_{\mathrm{CO_2}} k_2 (\mathrm{AsH})} \quad (13)$$

3. EXPERIMENTAL SECTION

3.1. Materials. The chosen amino sugars (purity 99%) were purchased from three local vendors in Mumbai: D-glucosamine hydrochloride from Molychem Chemicals, *N*-acetyl-D-glucosamine from Sisco Research Laboratories Pvt., Ltd., and *N*-methyl-D-glucamine from Sigma Aldrich Pvt., Ltd. The hydrochloride group in glucosamine was neutralized by adding sodium hydroxide in stoichiometric proportion. This neutralized form of glucosamine was used in all trials. MEA and PZ (purity 98%) were purchased from S. D. Fine Chemicals Pvt., Ltd., whereas AMP (purity 99%) was purchased from Molychem Chemicals. Inox Air Products Ltd., Mumbai, provided cylinders of pure CO_2, N_2, and nitrous oxide (N_2O).

3.2. Estimation of Solution Properties. Solution density was measured using a density meter (DMA 5000, Anton Parr). The viscosity of solutions of GA was measured using Ostwald's viscometer. Trials were performed using BSS number 3J-SIL borosilicate glass.

3.3. Stirred Cell Kinetics. The measurements were carried out with a jacketed stirred cell (diameter, 84 mm and height, 270 mm), with a volume of 1.48 L. The area of the flat gas–liquid interface was 55 cm^2. Before each experiment, N_2 was used to provide an inert atmosphere. The reactor was then evacuated, and 400 mL of the sugar solution was charged inside. Pure CO_2 was charged from a gas reservoir. The gas and liquid phases were stirred at 1000 and 60 rpm (accuracy = 1 rpm), and the fall in pressure was noted (accuracy = 1 mbar). Absorption rates were measured at 303, 308, and 313 K using the pressure versus time record.[15] The error in measuring rates (<2%) was found by repeating a few trials.

The gas-side mass-transfer resistance was neglected because the inert gas pressure was low, and the stirring speed was high.[16] The stirring speed (n) in liquid was raised from 60 to 100 rpm; yet, the absorption rates were identical. Thus, the value of k_L did not influence the rates, and the reaction was kinetically controlled. To validate the procedure for kinetic measurements, the rate constant for the CO_2–MEA system was measured at T = 303 K. Sada et al.[17] reported a value of 7740 M^{-1} s^{-1}, and our value was not too different (8015 M^{-1} s^{-1}). Thus, our experimental technique was validated.

4. RESULTS AND DISCUSSION

4.1. Properties of GA Solutions. The values of density and viscosity of aqueous GA solutions are represented in Table 1. The nonreactive N_2O gas is similar to CO_2 with regard to its molecular volume, electronic structure, and configuration. Thus, it can be used to estimate the properties of reactive CO_2.[18] The N_2O analogy method suggests that the ratio of the solubilities of CO_2 and N_2O remains constant for aqueous amines:

$$(\text{solubility of } \mathrm{CO_2}) = C_1(\text{solubility of } \mathrm{N_2O}) \quad (14)$$

where C_1 is given by

$$C_1 = \frac{(\text{solubility of } \mathrm{CO_2} \text{ in water})}{(\text{solubility of } \mathrm{N_2O} \text{ in water})} \quad (15)$$

The stirred cell was used for finding the N_2O solubility in GA solutions (H_{N_2O}). The values of solubilities of CO_2 and N_2O in water, earlier reported by Versteeg and van Swaiij,[18] were substituted in eq 15. The value of H_{CO_2} was then found using eq 14 (see Table 1). This anology can also be applied to estimate the diffusivity of CO_2 in solutions. The Stokes–Einstein relation and the value of N_2O diffusivity in water were used to find D_{N_2O} in GA solutions.[18] Using the value of D_{N_2O}, the diffusivity of CO_2 was found (see Table 1). More values of the solution properties over wider ranges of temperature (298–318 K) and GA concentration (20 mM–3 M) are listed in Tables S1–S6 in the Supporting Information. As evident from Table S2, GA solutions obey the common trend of rising viscosity with the

https://doi.org/10.1021/acs.iecr.2c02745
Ind. Eng. Chem. Res. 2023, 62, 1492–1498

growing solute concentration. When molarity is high (>1 M), GA solutions are clearly more viscous than water.

4.2. Liquid-Side Mass-Transfer Coefficient. The method of Littel et al.[19] was used for finding the value of k_L in the stirred cell. The equation for mass balance for CO_2 for both the gas and liquid phases, which was earlier derived in their work, was applied here:

$$\ln\left[\frac{P(t) - P_{final}}{P_{initial} - P_{final}}\right] = -\left[\frac{(\hat{m}V_L) + V_G}{V_L V_G}\right]k_L A t \quad (16)$$

From the study of physical absorption of CO_2 in water at 308 K and the pressure versus time record, a plot of $\ln\left[\frac{P(t) - P_{final}}{P_{initial} - P_{final}}\right]$ versus t was drawn. The values of $\hat{m}$ (= 0.28 mol/mol), V_G (= 1080 cm^3), V_L (= 400 cm^3), and A (= 55 cm^2) were known. From the value of the slope of this plot, viz., $\left\{-\left[\frac{(\hat{m}V_L) + V_G}{V_L V_G}\right]k_L A\right\}$, it was found that k_L equals 5×10^{-3} cm/s. This value is similar to that obtained by Patil et al.[5] and appears to be generally relevant for this model contactor. The value of k_L was corrected for the proposed solvent using the film theory correction factor ($k_L \propto$ diffusivity at any arbitrary temperature). The values of k_L at 303 and 313 K were found to be 4.9×10^{-3} and 5.4×10^{-3} cm/s, respectively.

4.3. Reaction Kinetics for GA. The rates of CO_2 absorption in aqueous GA solutions (0.1−1 M) were measured at 303, 308, and 313 K (see Table 2). The CO_2 partial pressure was around 5 kPa. The rates were higher in GA solutions of higher concentration. For example, the rate at 308 K increased from 1.03×10^{-7} (GA = 0.1 M) to 6.75×10^{-7} kmol m^{-2} s^{-1} (GA = 1 M). The rise in temperature also resulted in higher absorption rates. Thus, the rate of absorption in 1 M GA solution improved from 5.53×10^{-7} (T = 303 K) to 7.01×10^{-7} kmol m^{-2} s^{-1} (T = 313 K). Next, the dependence of rate on CO_2 partial pressure was studied in the 5−25 kPa range. A plot of R_{CO_2} versus P_{CO_2} at 308 K is shown in Figure 2 (GA = 0.5 M). This plot is linear, which verifies the first-order kinetics for CO_2. According to eq 12, $\log\left\{\frac{R_{CO_2}}{P_{CO_2}H_{CO_2}\sqrt{D_{CO_2}}}\right\}$ was plotted against log(GA) at 303, 308, and 313 K (see Figure 3). The values of the slope (0.8) suggested fractional reaction order (n = 1.6) with respect to the GA concentration. Earlier, the results of Gomez-Diaz and Navaza[3] suggested first-order kinetics for GA. It follows from eq 6 that this relation is valid: $[\hat{k}_{AsH}(AsH) + \hat{k}_{H_2O}(H_2O) + \hat{k}_{OH^-}(OH^-)] \ll k_{-1}$. Thus, zwitterion deprotonation is the rate-limiting step.

Table 2. Rates of CO_2 Absorption in Aq. GA Solutions (0.1−1 M) at 303, 308, and 313 K

temperature (K)	concentration (M)	CO_2 partial pressure (kPa)	rate of absorption × 10^7 (kmol/m^2 s)
303	0.1	5.07	0.89
	0.3	4.80	1.93
	0.5	4.53	2.57
	1	4.65	5.53
308	0.1	5.02	1.03
	0.3	4.52	2.25
	0.5	4.01	2.91
	1	4.87	6.75
313	0.1	4.76	1.11
	0.3	4.40	2.48
	0.5	4.04	3.23
	1	4.46	7.01

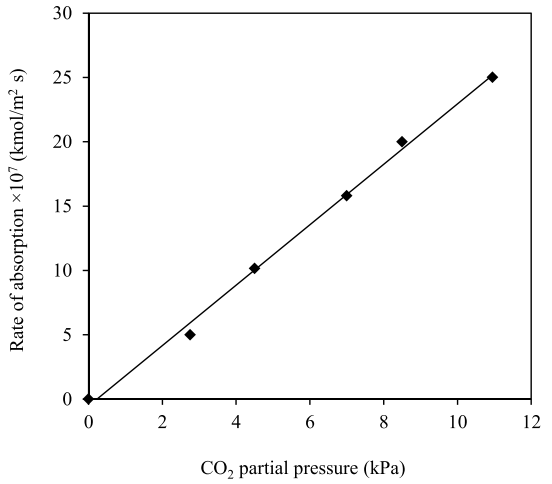

Figure 2. Plot of R_{CO_2} vs P_{CO_2} at T = 308 K (GA = 0.5 M).

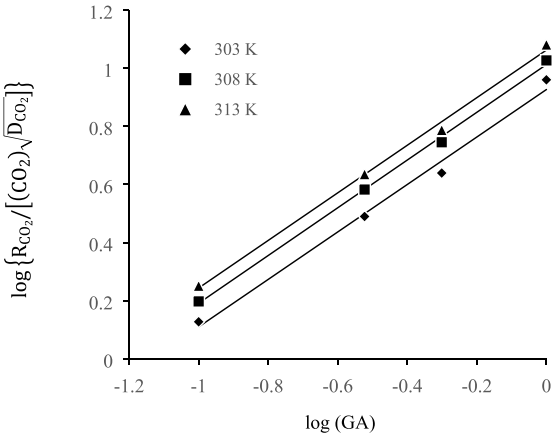

Figure 3. Plots of $\log\left\{\frac{R_{CO_2}}{P_{CO_2}H_{CO_2}\sqrt{D_{CO_2}}}\right\}$ vs log(GA) at 303, 308, and 313 K.

The kinetic data for GA solutions (0.1 M) at 303, 308, and 313 K are represented in Table 3. Using eq 13, the values of k_2 were found. The values of Ha and E_i suggest that the reaction is moderately fast. This is in line with the work of Gomez-Diaz and Navaza.[3] They also found that the CO_2−GA reaction is moderately fast (0.3 < Ha < 3). Thus, enhancement factor is given by the correlation $E = \sqrt{1 + Ha^2}$. The values of E are listed in Table 3. The variation in k_2 with temperature was studied. The Arrhenius plot is shown in Figure 4. The following correlation holds:

$$\ln(k_{2,GA}) = 23.749 - \left(\frac{6313.5}{T}\right) \quad (17)$$

The activation energy was 52 kJ mol^{-1}, which is close to the value published by Gomez-Diaz and Navaza[3] (47.6 kJ mol^{-1}).

4.4. Addition of Rate Promoters to GA. GA solutions (2.5 M) were promoted with three amines MEA, AMP, and PZ (0.5 M). It was recently reported that the chosen amines aided the absorption process in NAG solutions.[5] Experiments were performed at T = 308 K in the 5−25 kPa range of CO_2 partial

https://doi.org/10.1021/acs.iecr.2c02745
Ind. Eng. Chem. Res. 2023, 62, 1492−1498

Table 3. Kinetic Data on the CO_2−Aq. GA System at 303, 308, and 313 K (GA = 0.1 M)

temp. (K)	CO_2 partial pressure (kPa)	rate of absorption × 10^7 (kmol/m^2 s)	k_2 (M^{-1} s^{-1})	$k_L \times 10^3$ (cm/s)	Ha	E_i	$\sqrt{1+Ha^2}$
303	5.07	0.89	18	4.9	0.17	2.76	1.01
308	5.02	1.03	27	5.0	0.37	2.92	1.05
313	4.76	1.11	35	5.4	0.47	3.02	1.11

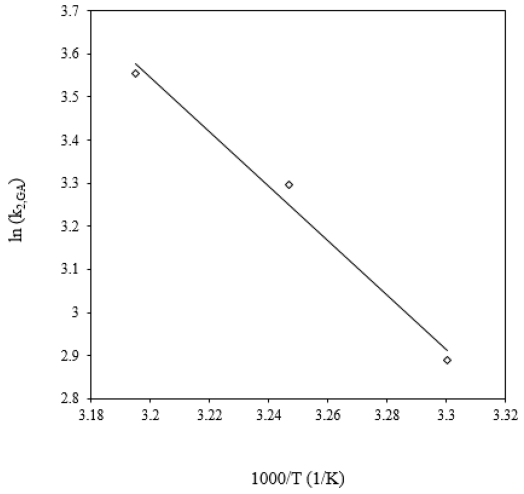

Figure 4. Arrhenius plot for the CO_2−GA system.

pressure. The results are represented in Figure 5. The rates improved with the rising partial pressure of CO_2. PZ was the most efficient promoter because the absorption rates in GA/PZ were the highest. All promoters form carbamates with CO_2. For all AsH/AmH mixtures (here, AmH denotes the promoter amine), eq 6 can be modified as follows:

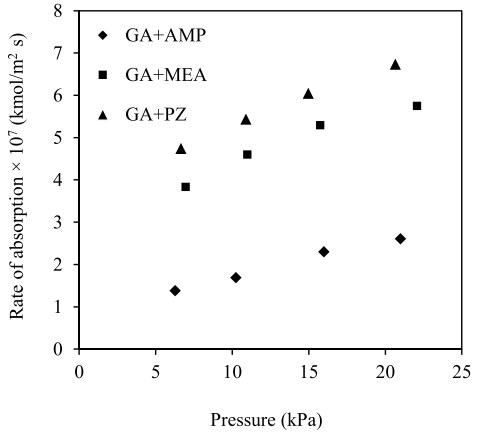

Figure 5. Dependence of R_{CO_2} on P_{CO_2} at 308 K for 2.5/0.5 M GA/promoter mixtures.

$$R_{CO_2} = \frac{k_{2,AsH}(CO_2)(AsH)}{1 + \frac{k_{-1,AsH}}{\hat{k}_{AsH}(AsH) + \hat{k}_{AmH}(AmH) + \hat{k}_{H_2O}(H_2O) + \hat{k}_{OH^-}(OH^-)}} + \frac{k_{2,AmH}(CO_2)(AmH)}{1 + \frac{k_{-1,AmH}}{\hat{k}_{AsH}(AsH) + \hat{k}_{AmH}(AmH) + \hat{k}_{H_2O}(H_2O) + \hat{k}_{OH^-}(OH^-)}} \quad (18)$$

Due to the high CO_2 reactivity of the promoter amines, deprotonation of the zwitterion is fast, and eq 18 can be simply rearranged as follows:

$$R_{CO_2} = k_{2,AsH}(CO_2)(AsH) + k_{2,AmH}(CO_2)(AmH) \quad (19)$$

4.5. Comparison of the Reactivity of GA, NAG, and NMG. Trials were performed in the stirred cell at 308 K using 0.5 M solutions of amino sugars. The value of the CO_2 partial pressure was around 4 kPa. From the measured values of the absorption rates (see Table 4), it was found that NMG was the most reactive with CO_2, whereas GA was the least reactive. As the results with NMG were encouraging, further trials were performed with this amino sugar. The rates of CO_2 absorption in aqueous NMG solutions (0.1−0.5 M) were measured at 303 and 308 K (see Table 5). In dilute solutions (sugar = 0.1 M), the absorption rate at T = 308 K and P_{CO_2}=8 kPa was low (R_{CO_2}=1.39 × 10^{-6} kmol/m^2 s). However, the rate in 0.3 and 0.5 M NMG solutions was markedly higher. Also, the rate at T = 308 K and (NMG) = 0.5 M was higher than the rate at 303 K, thus highlighting that the rise in temperature resulted in a higher absorption rate. In a forthcoming study, we will investigate the absorption kinetics in NMG solutions.

Table 4. Comparison of the CO_2 Reactivity of Amino Sugars (Molarity = 0.5 M) at 308 K

amino sugar	temperature (K)	sugar concentration (M)	CO_2 partial pressure (kPa)	rate of absorption × 10^7 (kmol/m^2 s)
GA	308	0.5	4.01	2.91
NAG	308	0.5	4.25	3.35
NMG	308	0.5	4.15	4.83

Table 5. Rates of CO_2 Absorption in Aq. NMG Solutions (0.1−0.5 M) at 303 and 308 K

temp. (K)	concentration of NMG (M)	CO_2 partial pressure (kPa)	rate of absorption × 10^6 (kmol/m^2 s)
303	0.5	7.98	3.86
308	0.1	7.69	1.39
	0.3	7.74	3.47
	0.5	8.85	6.10

4.6. Some General Remarks. The motive for the extra kinetic study performed in our work was to extend the scope of validity of the reported kinetic model of Gomez-Diaz and Navaza[3] to a high molarity of GA (up to 1 M) and find out the kinetic parameters (order, rate constant, or activation energy) and the reaction pathway (slowest step) in the 0.1−1 M range. A few of our outcomes (rate constant and E_{act}) matched well with the past work of Gomez-Diaz and Navaza[3] (molarity 0.05−0.4 M). However, we realized that kinetics was not of the first order for GA (n = 1.6), and the rate-limiting step was dissimilar (zwitterion deprotonation).

https://doi.org/10.1021/acs.iecr.2c02745
Ind. Eng. Chem. Res. 2023, 62, 1492−1498

Furthermore, we reported the physical properties of GA solutions (0.02−3 M) in the 298−318 K range because such data are hitherto not published. As a matter of fact, the properties of GA hydrochloride were systematically studied, but no work focused on GA at a high molarity. For example, Gomez-Diaz and Navaza[20] reported the density and viscosity of glucosamine hydrochloride (0−0.4 M) in the 298−323 K range. In another work, Gomez-Diaz et al.[1] presumed that carbon dioxide diffusivity and viscosity in the aqueous solutions of glucose and glucosamine are identical. There was no further information available, and we intended to fill this gap.

5. CONCLUSIONS

Amino sugars are potential solvents for CO_2 capture from industrial gases. In the present work, the absorption kinetics for glucosamine (GA) was investigated in a stirred cell reactor. The reaction orders for GA and CO_2 were determined. This reaction system corresponds to the moderately fast reaction regime. The physicochemical characterisitcs of GA solutions (20 mM−3 M) were measured between 303 and 313 K. The CO_2 reactivity of GA was low, and it was augmented by the addition of rate promoters MEA, AMP, and PZ. Rate enhancement was maximized upon the addition of PZ (0.5 M) to 2.5 M GA solutions. Next, the performance of two more amino sugars *N*-acetyl-D-glucosamine (or NAG) and *N*-methyl-D-glucamine (or NMG) was determined and compared to that of GA. The absorption rate for NMG was the highest among the chosen sugars. In this way, a proper insight into the efficacy of this class of compounds was provided.

■ ASSOCIATED CONTENT

Supporting Information

The Supporting Information is available free of charge at https://pubs.acs.org/doi/10.1021/acs.iecr.2c02745.

Physical property data for glucosamine (PDF)

■ AUTHOR INFORMATION

Corresponding Author

Prakash D. Vaidya − *Department of Chemical Engineering, Institute of Chemical Technology, Mumbai 400019, India;* orcid.org/0000-0001-5061-9635; Phone: +91 22 3361 2014; Email: pd.vaidya@ictmumbai.edu.in; Fax: +91 22 3361 1020

Authors

Urvashi K. Sarode − *Department of Chemical Engineering, Institute of Chemical Technology, Mumbai 400019, India*

Eugeny Y. Kenig − *Faculty of Mechanical Engineering, Chair of Fluid Process Engineering, Paderborn University, Paderborn D-33098, Germany*

Complete contact information is available at: https://pubs.acs.org/10.1021/acs.iecr.2c02745

Notes

The authors declare no competing financial interest.

■ ACKNOWLEDGMENTS

Urvashi Sarode is thankful to the Department of Science and Technology, New Delhi, for providing financial assistance [DST/TM/EWO/MI/CCUS/11(G) dated September 2019]. The authors acknowledge useful inputs received from Iman Hami Dindar and Dr. Nicole Lutters from Paderborn University.

■ NOMENCLATURE

A	interfacial area, m^2
AmH	amine used as an absorption activator
(AmH)	concentration of amine in liquid, M
AsH	amino sugar
(AsH)	concentration of amino sugar in liquid, M
(CO_2)	saturation concentration of CO_2, M
D_{AsH}	diffusivity of amino sugar in liquid, $m^2\ s^{-1}$
D_{CO_2}	diffusivity of CO_2 in liquid, $m^2\ s^{-1}$
E	enhancement factor due to chemical reaction
E_{act}	activation energy
E_i	enhancement factor for an instantaneous reaction
(GA)	initial concentration of GA in liquid, M
Ha	Hatta number
H_{CO_2}	solubility of CO_2 in liquid, kmol $m^{-3}\ kPa^{-1}$
(H_2O)	concentration of water, M
k_2	forward rate constant for the reaction between CO_2 and GA, $M^{-1}\ s^{-1}$
k_{-1}	reverse rate constant for the reaction between CO_2 and GA, $M^{-1}\ s^{-1}$
$\hat{k}_{AmH}$	deprotonation constant for amine
$\hat{k}_{AsH}$	deprotonation constant for amino sugar
$\hat{k}_{H_2O}$	deprotonation constant for water
k_L	liquid-side mass-transfer coefficient, $m\ s^{-1}$
$\hat{k}_{OH^-}$	deprotonation constant for OH^-
$\hat{m}$	dimensionless solubility, mol mol^{-1}
(OH^-)	hydroxyl ion concentration, M
P_{CO_2}	partial pressure of CO_2 in bulk gas phase, kPa
$P(t)$	partial pressure of solute gas at time t, kPa
P_{final}	final partial pressure of solute gas, kPa
$P_{initial}$	initial partial pressure of solute gas, kPa
(Promoter)	concentration of promoter in liquid, M
R_{CO_2}	absorption rate of CO_2, kmol $m^{-2}\ s^{-1}$
V_G	volume of gas phase, m^3
V_L	volume of liquid phase, m^3

Greek Symbols

ρ	density of amino sugar solution, $kg\ m^{-3}$
μ	viscosity of amino sugar solution, mPa s

■ REFERENCES

(1) Gomez-Diaz, D.; Navaza, J. M.; Sanjurjo, B.; Vazquez-Orgeira, L. Carbon dioxide absorption in glucosamine aqueous solutions. *Chem. Eng. J.* **2006**, *122*, 81−86.

(2) Garcia-Abuin, A.; Gomez-Diaz, D.; Navaza, J. M.; Vidal-Tato, I. CO_2 capture by aqueous solutions of glucosamine in a bubble column reactor. *Chem. Eng. J.* **2010**, *162*, 37−42.

(3) Gomez-Diaz, D.; Navaza, J. M. Kinetics of carbon dioxide absorption into aqueous glucosamine solutions. *AIChE J.* **2008**, *54*, 321−326.

(4) Garcia-Abuin, A.; Gomez-Diaz, D.; Navaza, J. M. Characterization of carbon dioxide capture by glucosamine: Liquid phase speciation and degradation. *J. Ind. Eng. Chem.* **2014**, *20*, 2272−2277.

(5) Patil, M. P.; Vaidya, P. D.; Kenig, E. Y. Kinetics of carbon dioxide removal using N-acetyl glucosamine. *ACS Omega* **2020**, *5*, 27043−27049.

(6) Liu, H.; Jiang, X.; Idem, R.; Dong, S.; Tontiwachwuthikul, P. Comprehensive reaction kinetics model of CO_2 absorption into 1-dimethylamino-2-propanol. *AIChE J.* **2022**, *68*, No. e17816.

(7) Moioli, S.; Ho, M. T.; Wiley, D. E.; Pellegrini, L. A. Assessment of carbon dioxide capture by precipitating potassium taurate solvent. *Int. J. Greenh. Gas Control* **2019**, *87*, 159−169.

(8) Moioli, S.; Pellegrini, L. A. Operating the CO_2 absorption plant in a post-combustion unit in flexible mode for cost reduction. *Chem. Eng. Res. Des.* **2019**, *147*, 604−614.

(9) Liu, H.; Jiang, X.; Idem, R.; Dong, S.; Tontiwachwuthikul, P. AI models for correlation of physical properties in system of 1DMA2P-CO_2-H_2O. *AIChE J.* **2022**, *68*, No. e17761.
(10) Quan, H.; Dong, S.; Zhao, D.; Li, H.; Geng, J.; Liu, H. Generic AI models for mass transfer coefficient prediction in amine-based CO_2 absorber, Part II: RBFNN and RF model. *AIChE J.* **2018**, *1*, No. e17904.
(11) Mahajani, V. V.; Joshi, J. B. Kinetics of reactions between carbon dioxide and alkanolamines. *Gas Sep. Purif.* **1988**, *2*, 50−64.
(12) Versteeg, G. F.; van Dijck, L. A. J.; van Swaaij, W. P. M. On the kinetics between CO_2 and alkanolamines both in aqueous and nonaqueous solutions. An overview. *Chem. Eng. Commun.* **1996**, *144*, 113−158.
(13) Vaidya, P. D.; Kenig, E. Y. CO_2-alkanolamine reaction kinetics: A review of recent studies. *Chem. Eng. Technol.* **2007**, *30*, 1467−1474.
(14) Doraiswamy, L. K.; Sharma, M. M. *Heterogeneous Reactions: Analysis, Examples and Reactor Design*, vol. 2; John Wiley and Sons: New York, 1984.
(15) Salvi, A. P.; Vaidya, P. D.; Kenig, E. Y. Kinetics of carbon dioxide removal by ethylene diamine and diethylene triamine in aqueous solutions. *Can. J. Chem. Eng.* **2014**, *92*, 2021−2028.
(16) Jiru, Y.; Eimer, D. A. A study of mass transfer kinetics of carbon dioxide in (monoethanolamine + water) in stirred cell. *Energy Procedia* **2013**, *37*, 2180−2187.
(17) Sada, E.; Kumazawa, H.; Han, Z. Q.; Matsuyama, H. Chemical kinetics of the reaction of carbon dioxide with ethanolamines in nonaqueous solvents. *AIChE J.* **1985**, *31*, 1297−1303.
(18) Versteeg, G. F.; van Swaaij, W. P. M. Solubility and diffusivity of acid gases (carbon dioxide, nitrous oxide) in aqueous alkanolamine solutions. *J. Chem. Eng. Data* **1988**, *33*, 29−34.
(19) Littel, R. J.; Versteeg, G. F.; van Swaaij, W. P. M. Physical absorption into non-aqueous solutions in a stirred cell reactor. *Chem. Eng. Sci.* **1991**, *46*, 3308−3313.
(20) Gomez-Diaz, D.; Navaza, J. M. Viscosimetric study of aqueous solutions of glucosamine and its mixtures with glucose. *J. Food Eng.* **2005**, *68*, 403−408.

https://doi.org/10.1021/acs.iecr.2c02745
Ind. Eng. Chem. Res. 2023, 62, 1492−1498